5th Australasian Congress on Applied Mechanics, ACAM 2007
10-12 December 2007, Brisbane, Australia

Simulation of vibrations produced by localized faults in rolling elements of bearings in gearboxes

N.Sawalhi[1] and R.B.Randall[1]

[1] *School of Mechanical and Manufacturing Engineering, The University of New South Wales, Sydney 2052, Australia*

Abstract: A combined gear/bearing model has been made to study the interaction between gears and bearings in the presence of faults. The thirty-four degree-of-freedom model of the University of New South Wales (UNSW) gearbox test rig is a lumped mass parameter model, which has the capacity to model different fault types (localized inner/outer race faults and extended faults). This is in addition to its original capacity for modelling spalls and cracks in the gears. The gear/bearing model takes into consideration the slippage in the bearings, the Hertzian contact and the nonlinearity of the bearing stiffness (time variant). Results have earlier been published for simulated local faults in the inner and outer races of the bearings as well as for an extended inner race fault. For a complete modelling of localized faults, the simulation model has now been updated to enable simulating faults in the rolling elements. The modeling of the faults in the rolling elements takes into consideration the difference in race curvature and represents a new contribution to the development of the model. The agreement between the processed simulated and measured signals shows the robustness of the developed model and its suitability for testing new diagnostic and prognostic algorithms.

Keywords: Envelope analysis, gear/bearing model, Hertzian contact, localized fault, rolling element bearing.

1 Introduction

In order to facilitate the development of diagnostic and prognostic techniques for rolling element bearings in real systems, a necessity existed to produce simulation models, where faults can be implemented under different operating conditions, rather than waiting for these to occur naturally, or alternatively having them seeded for laboratory testing.

This paper illustrates how to model localized faults in rolling elements in a gearbox environment. The paper is arranged as follows: After reviewing the dynamic simulation model of rolling element bearings [1] in section 2, the modelling of localized faults in rolling elements is discussed in section 3. A brief review of the UNSW gear/bearing model [1,2] is presented in section 4. The experimental and simulated results for a localized ball fault are compared and discussed in section 5.

2 Dynamic Simulation of rolling element bearings

Figure 1 illustrates the rolling element bearing-pedestal model, which has been derived and presented in [1]. The five degree-of-freedom model (5 DOF) is based on Hertzian contact theory [3], which relates the raceway displacement to the bearing load, and also accounts for the slippage between the elements. Forces in the horizontal (f_x) and vertical (f_y) directions are given in (1).

$$f_x = k_b \sum_{j=1}^{n_b} \gamma_j \delta_j^{1.5} \cos\phi_j , \qquad f_y = k_b \sum_{j=1}^{n_b} \gamma_j \delta_j^{1.5} \sin\phi_j \tag{1}$$

The load deflection factor k_b depends on the contact geometry and the elastic contacts of the material, the exponent n = 1.5 for ball bearings and 1.1 for roller bearings. The subscript j denotes the ball number and varies between 1 and n_b (total number of rolling elements). γ_j is a contact switch which accounts for the fact that compression occurs only for positive values. This is defined in (2) as:

$$\gamma_j = \begin{cases} 1, & \text{if } \delta_j > 0 \\ 0, & \text{otherwise} \end{cases} \tag{2}$$

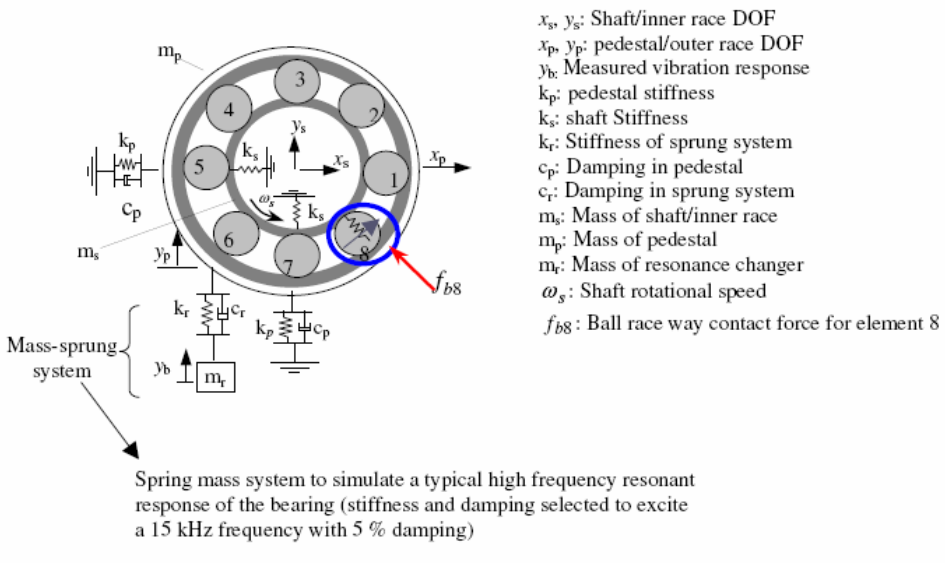

Figure 1 Five DOF bearing-pedestal model

The overall contact deformation (contact compression) for the *j*'th -rolling element δ_j is a function of the inner race displacement relative to the outer race in the *x* and *y* directions ($(x_s - x_p), (y_s - y_p)$), the element position ψ_j (time varying) and the clearance (c). This is given by:

$$\delta_j = (x_s - x_p)\cos\psi_j + (y_s - y_p)\sin\psi_j - c - \beta_j C_d \tag{3}$$

where ψ_j (angular position of the rolling element *j*) is defined in (4) as a function of the time increment dt, the previous cage position ψ_o and the cage speed ω_c and accounts for the slippage in the rolling elements (uncertainty in ball positions).

$$\psi_j = \frac{2\pi(j-1)}{n_b} + \omega_c dt + \overbrace{\psi_o}^{\text{preivous cage position}} + \overbrace{(0.5 - rand)\times\psi_{slip}}^{\text{slippage}} \tag{4}$$

β_j is a fault switch which simulates the contact loss at a defined angular position (ψ_d) over an angular distance of ($\Delta\psi_d$). The depth of the defect C_d was defined as a function of ψ so that a gradual rather than instant loss/gain of contact is achieved.

3 Modelling localized faults in rolling elements

A spall on one of the rolling elements (rolling element *k*) rotates at the same speed as the rolling element i.e. ω_{spin} (ball spin frequency), which is defined in (5) as:

$$w_{spin} = \frac{w_s}{2}\frac{D_p}{D_b}\left(1-\left(\frac{D_b}{D_p}\cos(a)\right)^2\right) \quad (5)$$

D_b is the rolling element diameter and D_p is the pitch diameter.

The position of the spall (f_s) can be defined as in (6)

$$f_s = w_{spin}\,t + f_{do} \quad (6)$$

where f_{do} : initial starting location of the spall.

The position of the spall is associated with the speed of the rolling element, which in turn is a function of the shaft speed. This means that the rolling element faults share some characteristics with faults on the inner race and exhibit a major difference from the faults associated with the outer race (fixed location).

The loss of contact is detected for only the faulty rolling element *k*, and this is done twice for each complete rotation of that rolling element, i.e. when it is in touch with the inner race and with the outer race. The switch values and the periods of switching on (Δf_d) will not be the same for both races, which results from the difference in curvature between the two races and is also a function of the rolling element diameter. The inner race will contact deeper and longer compared to the outer race. Instead of defining two spall geometries, the fault b_j switch can be modified to show this variation as sensed by the different races as in (7):

$$b_j = \begin{cases} 0, & j \neq k \\ 1, \quad \text{if } 0 < f_s < \Delta f_{do} & \\ \dfrac{C_{dr} + Cd_i}{C_{dr} - Cd_o} \text{ if } p < f_s < (p + \Delta f_{di}) & j = k \\ 0, \quad \text{otherwise} & \end{cases} \quad (7)$$

The derivation of the switch values is illustrated in Figure 2 (not to scale), when the spalled rolling element is in touch with the inner race. For this case, the total loss of contact - as a result of creating a slot of width $2x$ - is the summation of two values. The first is the maximum depth the inner race will enter in the slot region (C_{di} as calculated in (8), which represents the movement of the inner race from its original contact position - moving downwards*)*. The second represents the movement of the ball from its original contact position as a result of creating the slot (C_{dr} as presented in (9)- moving upwards).

Note that when the spalled element is in touch with the outer race, the net change in the contact (C_d) is the difference between the rolling element movement (C_{dr} *) and* outer race movement (C_{do}) as shown in (9) and (10) respectively. This is due to the fact that the outer race moves downwards and so does the rolling element, which means that the net change in the contact between the original and the new contact position can be obtained by subtracting the two changes.

$$C_{di} = r_i - \sqrt{r_i^2 - x^2} \quad (8)$$

$$C_{dr} = \frac{D_b}{2} - \sqrt{\left(\frac{D_b}{2}\right)^2 - x^2} \quad (9)$$

Similarly

$$C_{do} = r_o - \sqrt{r_o^2 - x^2} \quad \text{where } r_o = \frac{D_p + D_b}{2} \tag{10}$$

The angular widths of the fault will also depend on the race contacting the defective roller and are given by (11) for the outer (Δf_{d_o}) and inner (Δf_{di}) race contacts.

$$\Delta f_{d_o}(rad) = \frac{2 \times x}{ro} \quad , \quad \Delta f_{d_i}(rad) = \frac{2 \times x}{ri} \tag{11}$$

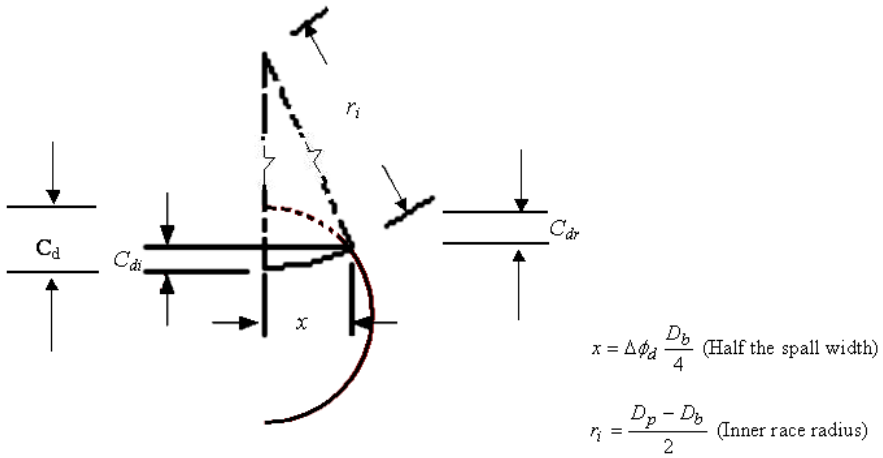

Figure 2 Rolling element spall depth as sensed by the inner race (not to scale)

4 The UNSW spur gear test rig model

A lumped mass parameter model (34 DOF model) was constructed to represent the different parameters of the UNSW gearbox test rig model (stiffness, damping and masses) in both translational and rotational degrees of freedom [2]. Both the 5-DOF bearing model and the gear model [4] were incorporated in the overall model. For a full and complete description of this model see reference [2]. Matlab® and Simulink® were employed to solve the set of the equations of motion. The bearing model was implemented as an S-function (special function for Simulink®), which was dynamically updated as the simulation proceeded. The load dependent non-linearity of the gearmesh stiffness was implemented as a "look-up table" with cubic spline interpolation [4].

5 Experimental and simulated results

A notch fault was introduced [5] into one of the rolling elements (balls) in a similar way to those introduced earlier to both inner and outer races using electric spark erosion [5]. The electrode was designed in such a way that the fault would extend over an included angle of 60° over the ball's surface. The generated gap in the ball has a rectangular cross-section (0.5 mm in depth and 0.5 mm wide). In the bearing simulation function, the width of the fault was set to 0.5 mm, while the depth was set to 10.7 μm when the ball touches the inner race and 7.4 μm when it touches the outer race (because of the respective convexity/concavity of the races). A preload value of –3 μm was used.

5.1 Time domain and power spectrum comparison

Figure 3 shows the accelerometer time domain signals for one complete rotation of the gears for both the simulated and measured signals. The pattern of the impacts in both simulation and measured signals is the same, except that in the simulation signal the impulses are more obvious and less damped. Note that the differences are much smaller in bandpass filtered signals given below.

To see the effect of the rolling element fault on the power spectra, both faulty simulated and the measured signals are compared with their fault free counterparts and the result is plotted in Figure 4. The rolling element localized fault is no exception to what has been previously [1,2] for the localized

faults in the inner and outer races. In both the simulation and the experimental cases, the localized ball defect excites the frequency region above 10 kHz. In the simulation, this is centred around the 15 kHz, while in the measured signal, it excites a wide range of the structure resonances as can be seen by the circled parts. These are responsible for the differences in time signals in Figure 3.

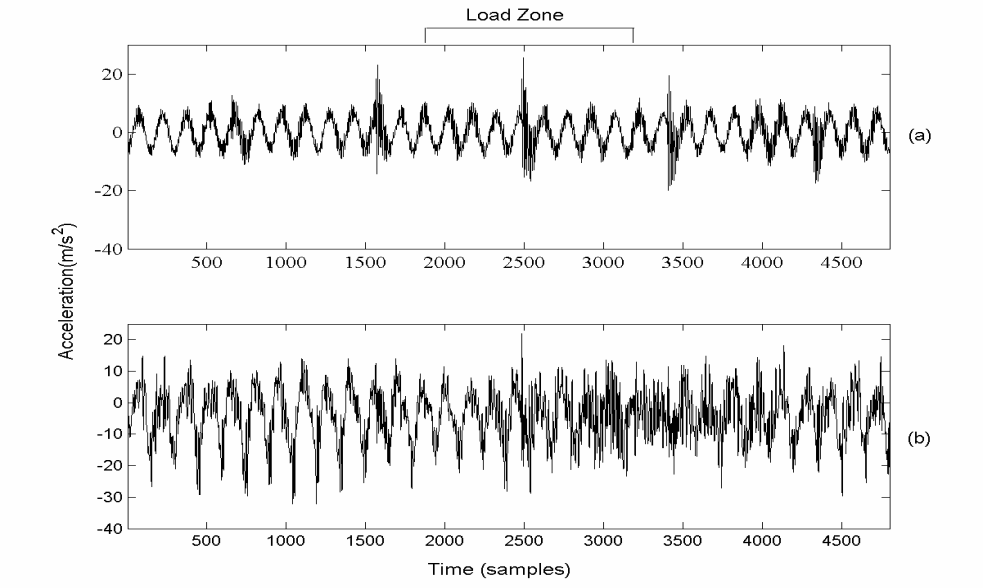

Figure 3 Time domain signals (a) Simulated (b) Measured

5.2 Envelope analysis

The signature of the rolling element faults is inspected through the filtered signals (obtained via the SK filter) and their corresponding squared envelope spectra. These are plotted in Figure 5 for the simulated and experimental cases, and show a much better agreement between the simulated and the actual signals than the unfiltered signals of Figure 3. The dominant frequency is (2x ball spin frequency (BSF)) (52 Hz) as the fault impacts twice during one complete rotation of the ball (on the inner and the outer races), which is modulated by the cage speed (4 Hz). Note also the existence of the BSF components in the squared envelope spectra for both the simulated and the measured signals. This is because of the variation of the impact severity between the inner and outer races; due to the difference in race curvature. If the defect depths were modelled to be the same for both the races, only harmonics of (2x BSF) would appear in the squared envelope spectra.

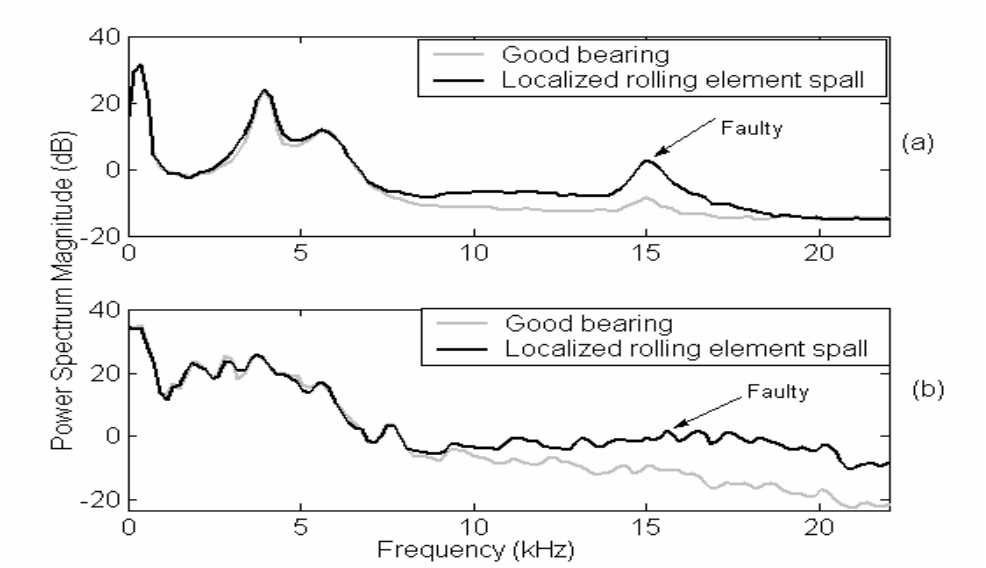

Figure 4 Power spectra comparison (a) Simulated (b) Experimental

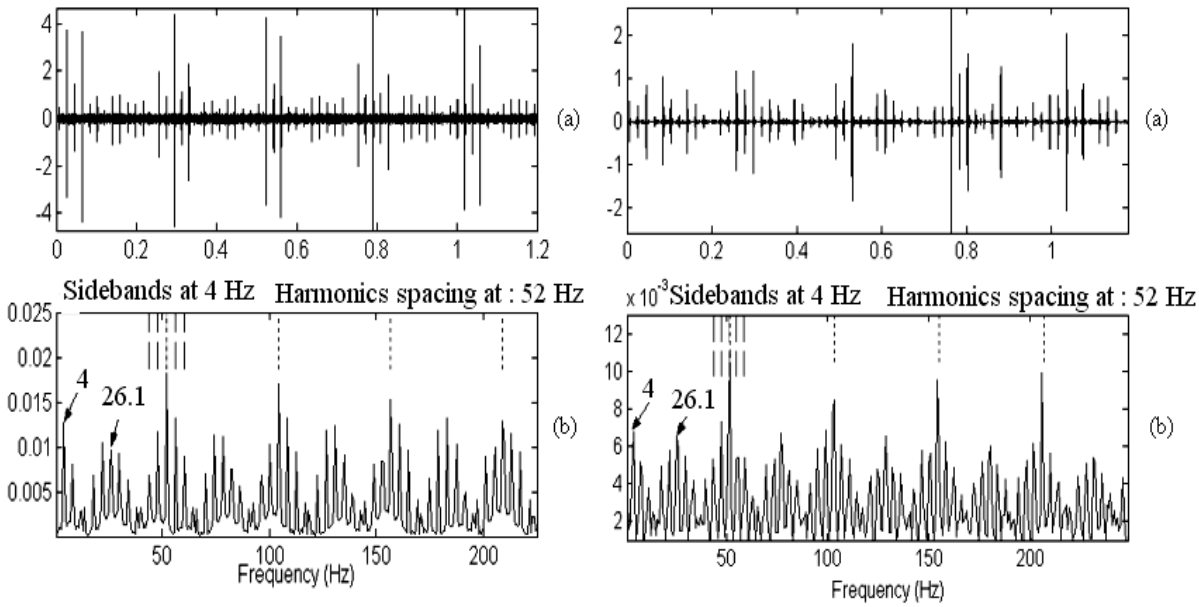

Figure 5 Envelope analysis for the localized rolling element fault. Left: simulated Right: experimental. (a) Filtered signals and (b) Squared envelope spectra

6 Conclusions

This paper presented a simulation model for a localized fault in a rolling element in one of the bearings of a single stage gearbox. The simulated fault produced signals, which are reasonably comparable to the measured ones. The simulated and measured signals reacted similarly to signal processing techniques normally applied to rolling element bearings (power spectrum comparison and envelope analysis). The similarity between simulated and measured signals subjected to diagnostic techniques suggests that the model can be used efficiently to simulate faults of different sizes and locations and could be quite useful in the development of prognostic methods.

7 Acknowledgments

This work is supported by the Australian Defence Science and Technology Organization (DSTO).

References

[1] Sawalhi, N., Randall R.B and Endo H. (2006): Simulating gear and bearing interactions in the presence of faults: paper presented at the 7th IFToMM Conference on Rotor Dynamics, Vienna, Austria, 25-28 September 2006.

[2] Sawalhi, N. (2007): *Diagnostics, prognostics and fault Simulation for rolling element bearings*. PhD Dissertation, UNSW, Sydney.

[3] Harris, F.J. (2000): Rolling Bearing Analysis II, John Wiley, New York.

[4] Endo, H. (2005): *A study of gear faults by simulation, and the development of differential diagnostic techniques*. PhD Dissertation, UNSW, Sydney.

[5] Ho, D. (1999): *Bearing Diagnostics and Self-Adaptive Noise Cancellation*. PhD Dissertation, UNSW, Sydney.